

Analyzing Free Space Optical Communication Performance

A. Ramezani, M. R. Noroozi, M. Aghababae

Abstract— Over the last three decades free-space optical communication (FSO) has become more and more interesting as an adjunct to radio frequency communication. In spite of the very great technical advancement of available components, the major limitation of free-space communication performance is due to the atmosphere, because a portion of the atmospheric path always includes turbulence and multiple scattering effects. Starting from a fundamental understanding of the optical communications system under different weather conditions, this paper provides a treatment of the evaluation of parameters needed for analyzing and simulation of system performance. Finally the advent of the new technology of wavelength division multiplexing (WDM) and a new compact laser communication terminal that increase the data rate and enhancing performance are explained.

Index Terms— Free Space Optical Communication (FSOC), wavelength division multiplexing (WDM), Link Budget, Turbulence, Fading.

I. INTRODUCTION

Although FSO is an old topic, due to the availability of advanced technologies and high requirement of broadband communications now, it becomes a new research area. The advantages of using FSO are no license required from Federal Communications Commission (FCC) for FSO installation. Apart from that, the cost of installation is principally economic because there is no extra cost of digging the street to lay fiber. In term of communication security, FSO uses narrow laser beam which makes detection, interception and jamming very difficult. Moreover, FSO hardware is also portable and quickly. There has been tremendous technical advancement of available components such as laser transmitter, high sensitivity optical receiver offering extremely high bandwidth, effective modulation techniques, improvement in low power consumption, weight, and size. In spite of many such development, the major limitation of free-space laser communication performance is the atmosphere. Atmospheric condition ultimately determines the optical communications systems performance not only of terrestrial applications but also for uplink-downlink, because a portion of the atmospheric path always includes turbulence and multiple scattering effects[1]. This paper provides a theoretical treatment, analysis and simulation of the performance of an optical communication system under a given communication format scheme.

Manuscript published on 30 October 2014.

* Correspondence Author (s)

A. Ramezani, Electrical & Electronics Engineering Department, Imam Khomeini Maritime Sciences University, Noshahr, Iran.

M. R. Noroozi, Electrical & Electronics Engineering Department, Imam Khomeini Maritime Sciences University, Noshahr, Iran.

M. Aghababae, Electrical & Electronics Engineering Department, Imam Khomeini Maritime Sciences University, Noshahr, Iran.

© The Authors. Published by Blue Eyes Intelligence Engineering and Sciences Publication (BEIESP). This is an [open access](http://creativecommons.org/licenses/by-nc-nd/4.0/) article under the CC-BY-NC-ND license <http://creativecommons.org/licenses/by-nc-nd/4.0/>

The performance of a system is mostly quantified by the “link margin”, i.e., the ratio, expressed in dB, of the signal power received to the signal power required to achieve a specified data rate with a specified acceptable probability of error. The link margin calculation is therefore necessary to design an acceptable system. Atmospheric conditions affect system performance and so need to be accounted for in the calculation. A link budget model has been developed that includes dependence on the atmospheric channel. This model aids designers in optimizing the optical station main parameters to be able to set up a data link with adequate performance. The main advantage in communicating with optical frequencies is the potential increase in information transfer rate. This rate is directly related to the bandwidth of the modulated carrier, which is generally limited to a fixed fraction of the carrier frequency itself. Therefore, increasing carrier frequency from RF or microwaves to optical waves increases the information capacity of a communication system by many orders of magnitude. A usable bandwidth at an optical frequency of ~ 200 THz will be about 10^5 times that of a carrier in the RF range. moreover, a longer wavelength necessitates a proportionately larger antenna to achieve the same gain. Because of these advantages, optical carrier frequencies can give very high data rates of 100 GHz or more [2]. In this paper an overview of the challenges a system designer has to respond to when implementing an FSO system is provided. In section 2, the overall system performance of a link is quantified using a link margin derived from the link equation and the effect of atmospheric turbulence to the link is discussed. In section 3, the achievable data rate be obtained and in section 4, the results of the performance enhancements are reported.

II. THE OPTICAL LINK EQUATION

The overall system performance of a link is determined using a link margin derived from the link equation. The optical link equation is analogous to the link equation for any radio frequency communication link. Starting with the transmit power the designer identifies all link losses and gains to determine the received signal level. The received signal level is then compared with the sensitivity of the receiver, thus giving the link margin.

A. Channel Without Atmospheric Disturbance

In this section optical links without atmospheric disturbance are discussed. In the basic free-space channel the optical field generated at the transmitter propagates only with an associated beam spreading loss. For this system the performance can be determined directly from the power flow.

The signal power received depends on the transmit power, transmit antenna gain, receive antenna gain, the range loss, and system dependent losses[2].

$$P_{RX} = P_{TX} \cdot G_{TX} \cdot G_R \cdot G_{R_{X, \text{system, line}}} \quad (1)$$

Assuming a Gaussian beam under filling the transmit aperture, the transmit antenna gain is given by [6]:

$$G_{TX} = \frac{32}{\Theta^2} \quad (2)$$

where Θ [rad] is the full-angle e^{-2} divergence of the transmit beam. The range loss G_r depends on the link propagation distance L and is given by[2]:

$$G_r = \left(\frac{\lambda}{4\pi L} \right)^2 \quad (3)$$

Further, the receive antenna gain, with telescope aperture diameter (antenna size) D , is given by [6]:

$$G_{RX} = \left(\frac{\pi D}{\lambda} \right)^2 \quad (4)$$

The $A_{\text{system, lin}}$ reflects all the other system-dependent losses. Because of the absence of atmospheric effects the link margin M_{link} in dB is given by:

$$M_{\text{Link[dB]}} = P_{RX, \text{dBm}} - S_r[\text{dBm}] \quad (5)$$

$S_r[\text{dBm}]$ is the required power at the receiver to achieve an expected communication performance, also called receiver sensitivity. It depends on data rate and the required bit error probability. Sensitivity depends on noise sources influencing the detection, such as ambient light and electronic noise. To consider the effects perturbing a link propagating through the Earth's atmosphere the link equation (5) must be extended. The primary atmospheric processes that affect optical wave propagation are extinction and refractive index turbulence (IRT). The principal problems of optical communication in the atmosphere are attenuation of optical intensity and fluctuations of received optical signal. An attenuation of optical intensity is caused by the absorption, scattering and refraction of optical waves by fog, snow and rain. Especially for short links heavy fog is the main factor that limits the link function. For link lengths exceeding several hundred meters fluctuations of received optical signal present a severe problem. Signal fluctuations of the received signal can in some time intervals fall below the receiver sensitivity S_r . In such time fading of the signal occurs. The effects of atmospheric extinction, atmospheric turbulence and fades are introduced in the following two sections.

B. Atmospheric Extinction Effect

Clouds, rain, snow, fog, haze, pollution etc. are atmospheric factors that affect our viewing of distant objects. These same factors also affect the transmission of a laser beam through the atmosphere. Atmospheric trace gases lead to strong and broad absorption bands, each consisting of a multitude of fine absorption lines. Based on the spectral distribution of these bands, the so called atmospheric optical transmission windows with low signal losses of the propagating beam can be calculated by evaluating thousands of absorption lines in the spectral range from $0.3\mu\text{m}$ to $14\mu\text{m}$. A description of the atmospheric transmission windows based on extensive evaluation of various data-bases, is given in Tab. 1, [12]. It can be seen that typical terrestrial communication wavelengths like 808 nm (Si detectors), 1064 nm (Nd-YAG lasers) or 1550 nm (InGaAs detectors, erbium-doped fiber amplifiers) are applicable, whereas 950 nm and 1300 nm are not ideal for FSO systems.

Table -1: Atmospheric Optical Transmission Windows (Window start- and stop-wavelength given in μm).

I	II	III	IV	V	VI	VII	VIII
0.3	0.97	1.16	1.4	1.9	3	4.5	7.7
.92	1.1	1.3	1.8	2.4	4.2	5.2	14

In addition to absorption, scattering has also to be taken into account. This can be described by the Rayleigh scattering coefficient [1]. Generally, scattering effects decrease with wavelength and altitude. Even in optical windows some extinction must be considered. A rough estimate for the clear-sky extinction is based on the parameter visibility V . This can be given by the Kruse relation. The Kruse relation, which is modified to reflect the attenuation in decibel per kilometer, is given by[2].

$$A_e[\text{dB/km}] = \frac{17}{V[\text{km}]} \cdot \left(\frac{0.55}{\lambda[\text{Hm}]} \right)^q \geq 0 \quad (6)$$

where the exponent q is given by

$$q = \begin{cases} 1.6 & V > 50 \text{ km} \\ 1.3 & 6 \text{ km} < V < 50 \text{ km} \\ 0.5850V^{\frac{1}{3}} & V < 6 \text{ km} \end{cases} \quad (7)$$

Coming back to the link equation, (5) must be modified by A_e [dB/km] in order to consider extinction effects of the atmosphere:

$$M_{\text{link}}[\text{dB}] = P_{RX, \text{dBm}} - S_r - L[\text{km}] \cdot A_e. \quad (8)$$

In the near-earth layer, rainfall and snow can also reduce the link margin and must be considered in the link equation (8). Several models exist to estimate the attenuation due to rainfall and snow.

C. Physical Effects of Optical Beam

Random variations of the refractive index, known as index-of-refraction turbulence (IRT) of the Earth's atmosphere are responsible for wave front distortion. Thus, if a beam with a longitudinal coherence length of at least several wavelengths propagates through IRT the intensity of the original beam profile is redistributed. Cross-sections of the beam before and after propagation through the atmosphere are shown in Fig. 1. As the refractive index structure along the path is time dependent because of the turbulent mixing of refractive index cells, the spatial intensity distribution at the receiver plane varies. The intensity scintillation-index σ_I^2 is the normalized variance of the intensity and is used as a measure of scintillations. The scintillation-index is usually evaluated in terms of the β_0^2 -parameter, which is an analytical measure for the integrated amount of turbulence along the link path.

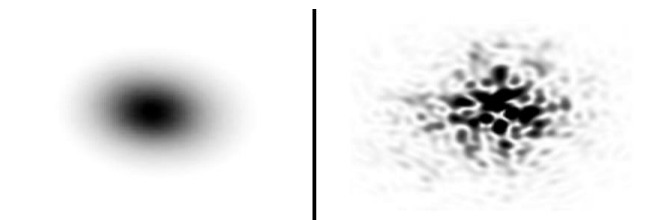


Fig. 1: Laser Beam Propagation through Turbulent Atmosphere: Intensity Cross-Section of the Transmit Beam (Left), Intensity Cross-Section at the Receiver Plane (Right) [2]

It shall be noted that for weak fluctuations ($\sigma_1^2 < 0.3$) the β_0^2 -parameter equals the Rytov variance. Fig. 3 shows the intensity scintillation index σ_1^2 as a function of β_0^2 of a spherical wave 1 under general irradiance fluctuation conditions 2. In strong turbulence or along long paths the scintillation-index saturates. Saturation occurs because multiple scattering can cause the incident wave to become increasingly incoherent as it propagates through the medium. A single source of light can, therefore, appear as extended multiple sources scintillating with random phase. When these multiple obvious source fields are added, the resultant intensity scintillation is limited [2]. Thus, for a low level of turbulence single scattering, which deflects light from the main beam, causes weak scintillation. For an increasing amount of turbulence more multiple scattering occurs. Multiple scattering can deviate light from the main beam but as turbulence gets stronger is can actually deflect the light back into the main beam again. Therefore the scintillation saturates. For a horizontal β_0^2 is given by [5]:

$$\beta_0^2 = 0.496 \cdot C_n^2 \cdot k^{\frac{7}{6}} \cdot L^{\frac{11}{6}} \quad (9)$$

Here, $k = \frac{2\pi}{\lambda}$ is the optical wave number and C_n^2 is the refractive index structure parameter. C_n^2 is the structure constant of refractive index fluctuations and a measure of the turbulence strength, given in $m^{-2/3}$. It depends strongly on the height above ground h_a . The Hufnagel-Vally model provides a model often used by researchers to describe the altitude dependence of $C_n^2(h_a)$ in rural areas. The H-V_{5/7} variant of the Hufnagel-Vally model is given by [7].

$$C_n^2(h_a) = \frac{9}{853} \times 10^{-18} + \frac{4}{9877} \times 10^{-6} \exp\left(-\frac{h_a}{300}\right) + \frac{2}{9228} \times 10^{-16} \exp\left(-\frac{h_a}{1200}\right) \quad (10)$$

Height dependent values of C_n^2 based on the H-V_{5/7} model are given in Fig. 2. The Hufnagel-Valley model gives an averaged C_n^2 value for a certain altitude. IRT above water differs from that above soil due to the fact that energy conversion on the ground is controlled almost exclusively by molecular conduction. In water, however, there is an additional exchange of mass and heat transfer at the air-water interface by convection, advection and evaporation. The potential rate of evaporation is determined by the air-sea temperature difference and the state of the air.

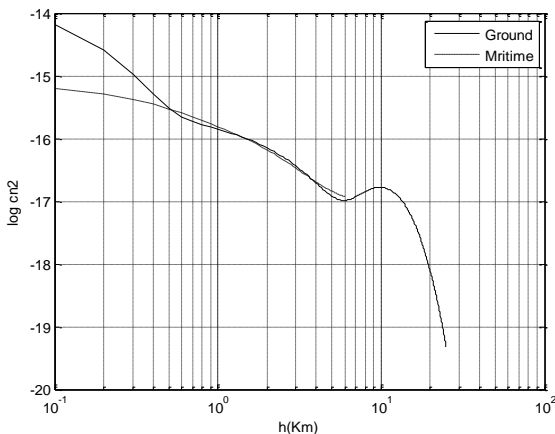


Fig. 2 Rural C_n^2 as a Function of High Above Ground h in Comparison with a Maritime- C_n^2 Model

Because of the large thermal capacity of water, it requires

much more energy to raise the temperature of a volume of water than for most soils, Therefore air-sea temperature difference is smaller than the temperature difference between most other natural surfaces. Furthermore, the daily fluctuations of the water surface temperature will be small. In general, the C_n^2 values above water are smaller than expected above land. Majumdar provides in his work a maritime turbulence profile model for altitudes up to 6000m. The model is in good agreement with the measured values. The medium profile maritime C_n^2 model, which is valid for $h_a < 6000$ m is given by as [6].

$$C_n^2(h_a) = \frac{9}{853} \times 10^{-18} + \frac{4}{9877} \times 10^{-6} \exp\left(-\frac{h_a}{300}\right) + \frac{2}{9228} \times 10^{-16} \exp\left(-\frac{h_a}{1200}\right) \quad (11)$$

This maritime C_n^2 profile is shown in Fig. 2 in comparison with the rural H-V_{5/7}-model. It can be seen that above 500 m there is not much difference between the two models, because the influence of the boundary layer is negligible.

D. Reception of Distorted Wave Front

Atmospheric propagation disturbs the beam profile, which means that the wave front of the optical beam is distorted. Receiving this distorted wave front will cause signal fading. The fading effect are discussed in this section. In optical receiver systems the energy in the beam is collected by a receive aperture. We consider circular receiver apertures defined by the function [7].

$$f_{Ra}(r, D) = \begin{cases} 1, & \text{if } |r| \leq \frac{D}{2} \\ 0, & \text{if } |r| > \frac{D}{2} \end{cases} \quad (12)$$

where D is the diameter of the receiver aperture. It is typically in the range of several centimeters to tens of centimeters. r is the radial distance from the optical axis. We assume long-range communication links, where the optical signal spot at the receiver plane is several times larger than the aperture diameter D .

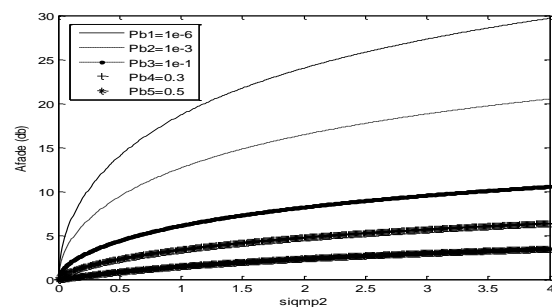


Fig. 3 Fading Loss vs. Power Scintillation-Index as a Function of Fractional Fade Time

In this case the received signal amplitude equals the integral of optical intensity $I(r; t)$ over area [7].

$$P_{Rx}(t) = \int \int_{-\infty}^{\infty} f_{Rx}(r, D) \cdot I(r, t) d^2r \quad (13)$$

The effect of integrating over the intensity reduces the deleterious effects of scintillation. This reduction is called aperture averaging. Within each region the scintillations are perfectly correlated while between the regions there is no significant correlation.

The regions are also called speckle. For horizontal paths a rough estimate for the speckle size at the receiver is given by the communication wavelength and the link distance [6]. If the aperture is larger than the speckle size, then uncorrelated scintillations from many regions will be averaged together, thereby reducing the signal dynamics. As can be observed in Fig. 3 the fading loss can easily exceed 20 dB with typical link requirements. Further, for moderate requirements with turbulence saturation the loss will rarely exceed 12 dB. Saturation means that for long distances the intensity scintillation index σ_I^2 is saturated near unity while the power scintillation-index becomes less than unity because of aperture averaging [9]. Finally, having introduced all the main factors perturbing a free-space optical link inside the atmosphere we can calculate link budget. An example link budget for a 20 km horizontal link is shown in Fig. 6. Further we evaluate the influence of IRT induced fading-loss versus link range. Therefore we chose the following link parameter:

$$\lambda=1550\text{nm} , \theta = 1 \text{ mrad} , D = 5 \text{ cm} ; l_{in} = 0.5, \\ P_{Tx} = 500 \text{ mW} , S_r = -43 \text{ dBm}, B= 155\text{Mbit/s} \\ , p_B = 0.01C_n^2(h = \text{Constant}) = 1 \times 10^{-4} \text{m}^{-2/3} \\ A_e = 0.2 \text{ dB/km}$$

Fig. 4 shows the link margins according to (9). With increasing link length the integrated amount of turbulence increases. This first causes the scintillation-index to increase steadily, then a maximum is observed and finally it saturates. As shown in the lower plot in Fig. 4, the fading-loss behaves in a way analogous to the scintillation-index. It first increases, peaks, and is then nearly constant for longer distances.

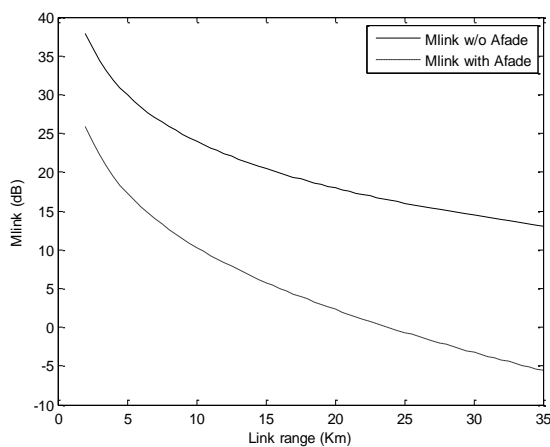


Fig. 4 Link Margin Including the Effect of Fading Cause by IRT in Comparison to a Case without Atmospheric Fading

III. DATA RATE ANALYSIS

The ability to predict system performance is essential for the design of a practical, optimal, cost-effective system. The FSO system must be able to establish a communication link between transmitting and receiving stations with a specified data rate and a probability of error lower than a specified bit-error rate (BER). Given a laser transmitter power P_t , with transmitter divergence of θ_t , receiver telescope area A , transmit and receive optical efficiency τ_{opt} , the achievable data rate R can be obtained from:

$$R = \frac{P_t \tau_{opt} \tau_{ATM} A}{\pi (\theta_t / 2)^2 L^2 E_p N_b} \quad (14)$$

Where τ_{ATM} is the value of the atmospheric transmission at

the laser transmitter wavelength, $E_p = hc/\lambda$ is the photon energy and N_b is the receiver sensitivity in # photons/bit. The range equation can be used to generate the communications data rate versus range for varying atmospheric conditions. Suppose a 2.5-km link is desired at 1.25Gbit/s. Furthermore, the system has to be eye safe, so that we use a 1.55- μm laser with 70mW power. We assume a 13-cm receiver aperture and transmitting beam divergence of 8.5mrad FWHM. Receiver sensitivity for 1.25Gbit/s was taken to be -36dBm, which is equivalent to 1568 photons/bit at this wavelength and data rate. Based on these assumptions, link margins were calculated for signal attenuation due to weather events such as clear (visibility= 23 km, $\alpha = 0.2$ dB/km), haze (visibility = 2 km, $\alpha = 4$ dB/km), and fog (visibility = 0.5 km, $\alpha = 21$ dB/km). The transmitter and receiver optics efficiencies are both assumed to be equal to 0.5 [1]. Data rates versus range is shown in Fig. 5. As can be seen, a data rate of 3Gbit/s can be achieved for a range of 2.4 km under clear condition, for 1.4 km under haze condition, and for 0.6 km under fog condition. The system is desired to have communication capability for the above ranges and atmospheric conditions. Under night-time conditions, the ranges would be increased further. Increased data rate is possible if a higher power laser, or a larger aperture, or both, is used.

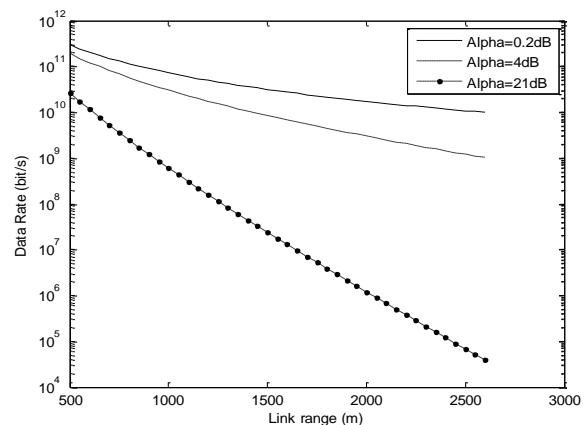


Fig. 5 Communication Data Rate as a Function of Range for Three Atmospheric Conditions: Clear ($\alpha = 0.2$ dB/km), Haze ($\alpha = 4$ dB/km) and Fog ($\alpha = 21$ dB/km)

IV. DEVELOPMENT OF A FSO

In this information age, the demand for high speed, high bandwidth communications channel, is ever increasing. FSO is presented as a solution to these demands in that it is free to implement, easy to install and of very high bandwidth. In this section, we explain two methods for increasing bandwidth and reducing of turbulence of atmosphere.

A. WDM System In FSO

In a Wavelength Division Multiplexing (WDM)-based access, the requirement for bandwidth has increased in an extremely fast and is a promising solution for data transport in future all-optical wide area networks. At the same time, the cost of transporting information bit per km also needs to be reduced.

WDM system in Free Space Optical, according fig. 6, is the way to maximize the bandwidth usage but in low cost. It has been quite mature and applied to optical fiber networks universally. Several FSO WDM transmission system have been demonstrated successfully (Kintaka et al., 2010 and Sinefeld and Marom, 2010). WDM is a technology which multiplexes multiple optical carrier signals on a single medium by using different signals. It is the technique to carry many separate optical signals. Each signal modulated into different wavelength lasers and it transmitted at a different rate from the other signal [3].

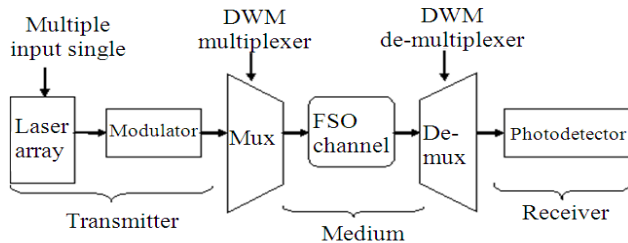


Fig. 6 Block Diagram of WDM System in FSO Transmission [3]

A. Performance Enhancements Against Atmospheric Turbulence

A new FSOC terminal according fig.7, designed. To Provide flexible and high speed connectivity to the terrestrial FSOC,

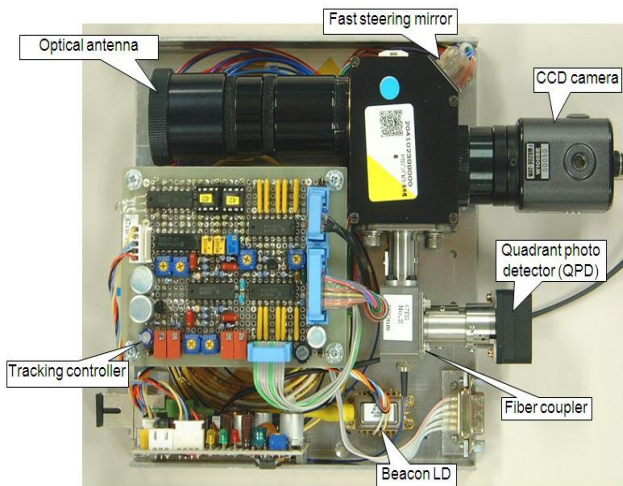


Fig-7 Internal Layout of the Compact FSO Terminal [4]

A new compact laser communication terminal has been developed at NICT. The terminal has a feature to connect the free-space laser beam directly to single mode fiber by using a special fiber coupler to focus the free-space laser beam and couple it into the single mode fiber, fast and accurate fine tracking system and a small refractive-type telescope with diffraction limited performance. The effect of atmospheric turbulence to the link quality with the fine tracking system is discussed and the results of the performance enhancements are also reported [4].

V. CONCLUSIONS

The advantages of FSO result from the basic characteristics of a laser beam which lead to efficient delivery of power to a receiver and a high information-carrying capacity. The main problems of FSO links working in the atmosphere result from attenuation and fluctuation of optical signal at a receiver. The effect of atmospheric turbulence to the link quality is

discussed and the results of the link quality enhancements have been reported. It is clear that FSO has good prospects for widespread implementation. FSO technology is ready for utilization as terrestrial links, mobile links and satellite links. It is obvious that the free space optical communication is here to stay. With our increased knowledge of atmospheric effects and the physics of turbulence generation and interactions with optical waves, and the continuous push for developing more sensitive receivers, FSOC system performance will continue to improve, with increasingly higher data rates, accuracy, and availability under all-weather atmospheric conditions.

REFERENCES

- [1] Arun K. Majumdar. Free-space laser communication performance in the atmospheric channel. J. Opt. Fiber. Commun. Rep. 2, 345-396© 2005 Springer Science Business Media Inc.
- [2] Hennes HENNIGER1, Otakar WILFERT2, An Introduction to Free-space Optical Communications RADIOENGINEERING, VOL. 19, NO. 2, JUNE 2010
- [3] Salasiah Hitam, Siti Norziela Suhaimi, Ahmad Shukri Mohd Noor, Siti Barirah Ahmad Anas and Ratna Kalos Zakiah Sahbudin. Performance Analysis on 16-Channels Wavelength Division Multiplexing in Free Space. Optical Transmission under Tropical Regions Environment. Journal of Computer Science 8 (1): 145-148, 2012 ISSN 1549-3636© 2012 Science Publications.
- [4] Yoshinori Arimoto. Compact free-space optical terminal for multi-gigabit signal transmissions with a single mode fiber. Free-Space Laser Communication Technologies XXI, edited by Hamid Hemmati, Proc. of SPIE Vol. 7199, 719908 · © 2009 SPIE
- [5] DAS, S., HENNIGER, H., EPPLER, B., MOORE, C., RABINOVICH, W., SOVA, R., YOUNG, D. Requirements and challenges for tactical free-space laser comm. In IEEE Military Communications Conference. San Diego (USA), 2008.
- [6] MAJUMDAR, A. K., RICKLIN, J. C. Free-Space Laser Communications Principles and Advances. Sew York (USA): Springer, 2008.
- [7] GIGGENBACH, D., HENNIGER, H. Fading-loss assessment in atmospheric free-space optical communication links with on-off keying. Optical Engineering, 2008.
- [8] MAYER, B., SHABDANOV, S., GIGGENBACH, D. Atmospheric Database of Atmospheric Absorption Coefficients (technical report). German Aerospace Center (DLR), 2002.
- [9] WILFERT, O., KOLKA, Z. Statistical model of free-space optical data link. Proceedings of SPIE, 2004, vol. 5550, p. 203 – 213.
- [10] Daniel V. Hahn, David M. Brown, Andrea M. Brown, Chun-Huei Bair, Mark J. Mayr, Nathan W. Rolander, Joseph E. Sluz, and Radha Venkat. Fog Conformal Free-Space Optical Communications Terminal Designs for Highly Confined Vehicles. JOHNS HOPKINS APL TECHNICAL DIGEST, VOLUME 30, NUMBER 4 (2012)
- [11] S. Qhumayo, R. Martinez Manuel. Free Space Optical data communication link. Photonics Research Group, Department of Electronic and Electrical Engineering University of Johannesburg, PO Box 524, Auckland Park, 2006
- [12] EDWARDS, D. P. GENLN2: A General Line-by-Line Atmospheric Transmittance and Radiance Model. Version 3.0: Description and users guide (technical report). National Center for Atmospheric Research, 1992.



Ali Ramezani, was born on 1980, in Arak, Iran. He received the B.Sc. and M.Sc. degrees in Electrical and Electronic Engineering from the Imam Khomeini Maritime Sciences University and Iran University of Science & Technology, in 2003 and 2006 respectively. Currently, he is the Ph.D. student in the Electrical and Electronic Engineering at the Isfahan University of Technology. Since 2006, he is a faculty member of Electrical and Electronic Engineering at Imam Khomeini Maritime Sciences University, Noshahr, Iran. His research interests are Digital Signal Processing, Digital Communication, Sonar Imaging and Radar Applications.





Mohammad Reza Noroozi, was born on 1974, in Arak, Iran. He received the B.Sc. and M.Sc. degrees in Electrical and Electronic Engineering from the Imam Khomeini Maritime Sciences University and Islamic Azad University, in 1998 and 2005 respectively. Currently, he is the Ph.D. student in the Electrical and Electronic Engineering at the Iran University of Science and Technology, Tehran, Iran. Since 2000, he is a faculty member of Electrical and Electronic Engineering at Imam Khomeini Maritime Sciences University, Noshahr, Iran. His research interests are Digital Signal Processing, Digital Image Processing, Sonar Imaging and Radar Applications.



Majid Aghababae, was born on 1971, in Tehran, Iran. He received the B.Sc. and M.Sc. degrees in Electrical and Electronic Engineering from the Sharif University of Technology, Tehran, Iran in 1992 and 1995 respectively. Currently, he is the assistant professor in the Electrical and Electronic Engineering at the Imam Khomeini Maritime Sciences University, Noshahr, Iran. His research interests are Digital Signal Processing, Digital Image Processing, Sonar Imaging and Radar Applications.